Title

SRSF2 Is Essential For Hematopoiesis and Its Mutations Dysregulate Alternative RNA Splicing In MDS

Journal

Blood, 122(21)

ISSN

0006-4971

Authors

Komeno, Yukiko
Qiu, Jinsong
Lin, Leo
et al.

Publication Date

2013-11-15

DOI

10.1182/blood.v122.21.261.261

Peer reviewed

SRSF2 is essential for hematopoiesis and its myelodysplastic syndromes-related mutations dysregulate alternative pre-mRNA splicing

Yukiko Komeno,[a,*] Yi-Jou Huang,[b,*] Jinsong Qiu,[c] Leo Lin,[b] YiJun Xu,[b] Yu Zhou,[c] Liang Chen,[c] Dora D. Monterroza,[b] Hairi Li,[c] Russell C. DeKelver,[b] Ming Yan,[a] Xiang-Dong Fu,[a,c,#] and Dong-Er Zhang[a,b,d,#]

Moores UCSD Cancer Center, University of California San Diego, La Jolla, CA, USA[a]; Department of Cellular and Molecular Medicine, University of California San Diego, La Jolla, CA, USA[b]; Division of Biological Sciences, University of California San Diego, La Jolla, CA, USA[c]; Department of Pathology, University of California San Diego, La Jolla, CA, USA[d]

Running Head: SRSF2 in hematopoiesis and MDS

* Co-first authors

Address correspondence to Dong-Er Zhang, dez@ucsd.edu; Xiang-Dong Fu, xdfu@ucsd.edu

Materials and Methods, 7780 characters

Combined word count for the Abstract, Introduction, Results, Discussion and Figure Legends sections, 30719 characters

Abstract

Myelodysplastic syndromes are a group of neoplasms characterized by ineffective myeloid hematopoiesis and various risks for leukemia. SRSF2, an SR family member of splicing factors, is one of the mutation targets associated with poor survival in patients of myelodysplastic syndromes. Here we report the biological function of *SRSF2* in hematopoiesis on conditional knockout mouse models. Ablation of *SRSF2* in the hematopoietic lineage caused embryonic lethality, and *Srsf2*-deficient fetal liver cells showed significantly enhanced apoptosis and decreased hematopoietic stem/progenitor cells. Induced ablation of *SRSF2* in adult *Mx1Cre*/ *Srsf2*flox/flox mice upon polyinosinic:polycytidylic acid injection demonstrated a significant decrease in lineage-/Sca+/cKit+ cells in bone marrow. To reveal the functional impact of myelodysplastic syndromes-associated mutations in *SRSF2*, we analyzed splicing responses on a MDS-L cell line and found that the P95H missense mutation and P95 to R102 in-frame 8 amino-acid deletion caused significant changes in alternative splicing. The affected genes were enriched in cancer development and apoptosis. These findings suggest that intact SRSF2 is essential for the functional integrity of the hematopoietic system, and its mutations likely contribute to development of myelodysplastic syndromes.

Introduction

Multiple classes of genetic aberrations have been suggested as the cause of myelodysplastic syndromes (MDS) (1, 2), including mutations in signal transduction, transcription factors, and epigenetic modifiers (3-5). Interestingly, recent genome-wide sequencing studies reveal that mutations in genes encoding splicing factors are commonly associated with MDS and other hematological malignancies (6-15). One of these newly identified genes encodes for the splicing factor SRSF2 (also known as SC35), and its mutations have been linked to poor survival among MDS patients (16, 17). Most of the *SRSF2* mutations occurred at proline 95, and the majority of these mutations changed this proline to histidine (P95H); less frequent changes to leucine (P95L), arginine (P95R), and in-frame deletion of 8 amino acids from P95 to R102 (Δ8aa) have also been reported (6, 16, 18-20). However, the causal effect of these mutations on MDS development has remained to be established.

SRSF2 is one of the founding members for the SR protein family of splicing factors (21). It is involved in both constitutive and regulated splicing. Homozygous germline knockout (KO) mice of *Srsf2* are embryonic lethal (22), and conditional knockout (cKO) mice display various tissue-specific phenotypes (22-24). Importantly, *Srsf2* down-regulation in mouse embryonic fibroblasts results in G2/M cell cycle arrest and genomic instability (23). To date, systematic analysis of SRSF2 function in the blood system has not been reported except for its requirement in T-cell development (24). Given the tight link of *Srsf2* mutations to MDS, we aim to directly test the hypothesis that SRSF2 plays an important role in normal hematopoiesis, and that *SRSF2* mutations induce specific changes in alternative splicing that favor disease progression.

Here we analyzed SRSF2 function in hematopoiesis on two mouse models by crossing cKO mice with blood cell-specific *Vav-iCre* mice and interferon-inducible *Mx1Cre* mice. We also generated an inducible shRNA/cDNA expression system to replace endogenous SRSF2 with specific mutants in a MDS cell line to evaluate the splicing response to mutant SRSF2 by RNA-mediated oligonucleotide annealing, selection, and ligation coupled with next-generation sequencing (RASL-seq) (25, 26). We report that SRSF2 is essential for the survival of hematopoietic cells in developing embryos and adults, and that its mutant forms switch the RNA splicing profile on a large panel of genes involved in cancer development and apoptosis. Together, these data suggest that *SRSF2* mutations identified in MDS are not simply loss-of-function mutations but instead alter SRSF2 function in RNA splicing. Such changes may directly contribute to MDS development and later progression to more aggressive forms of leukemia.

Materials and Methods

Mice

C57BL/6 (CD45.2), congenic strain B6.SJL-*Ptprc*^{a} *Pep3*^{b}/BoyJ (PEP3, CD45.1) mice, *Vav-iCre* and *Mx1Cre* mice were obtained from Jackson Laboratory. Conditional *Srsf2*$^{f/f}$ mice of C57BL/6 background were described previously (24). For embryo analyses, *Srsf2*$^{f/f}$ mice were mated with *Vav-iCre* +*Srsf2*$^{f/+}$ mice. To collect peripheral blood, embryos were bled from umbilical cord into PBS. Fetal livers from embryonic day 14.5 (E14.5) were fixed in 4% formaldehyde/PBS, and the tissue section was stained with Hematoxylin-Eosin. Polyinosinic:polycytidylic acid (Poly IC, Sigma) was injected intraperitoneally (*i.p.*) either 250 μg/body every other day for a total of 3 injections or 600 μg/body as indicated. Age-matched adult mice (8 -12 weeks old) were used for experiments. The day of the first injection was defined as day 0. Both protocols resulted in similar knock-down efficiency. Genotyping PCR was performed using primers described previously (23). All the procedures were approved by the institutional animal care and use committee.

DNA Constructs

C-terminally HA-tagged human *SRSF2* was subcloned in the EcoRI site of MSCV-IRES-GFP (MigR1) , MSCV-IRES-puro (MIP), and pREV-TRE (23). P95H and Δ8aa mutants were made by PCR mutagenesis. Primers used for mutagenesis are as follows. P95H(F): CAAATG GCGCGCTACGGCCGCCACCCGGACTCACACCACAGCCGC. P95H(R): GCGGCTGTGGTGTGAGTCCGGGTGGCGGCCGTAGCGCGCCATTTG. Δ8aa(F): CGGGTGCAAATGGCGCGCTACGGCCGCCGGGGACCGCCACCCCGC AGGTACGGGG.

Δ8aa(R): CCCCGTACCTGCGGGGTGGCGGTCCCCGGCGGCCGTAGCGCGCCA TTTGCACCCG. pTRIPZ-*SRSF2* constructs were made using shRNA against the 3'-UTR of human WT *SRSF2* (CTCTCCCGATTGCTCCTGTGTA) and human *SRSF2* cDNA sequences with or without mutations.

Cell culture

293T cells, mouse fetal liver (FL) cells (E12.5-E14.5), total BM cells and lineage-depleted BM cells (sorted by using Lineage depletion kit from Miltenyi) were cultured as described before (27). To make single cell suspension of FL cells, FLs were sheared in PBS by pipetting, passed through 40 μm cell strainers, and treated with ACK buffer [150 mM NH_4Cl, 1 mM $KHCO_3$, 0.1 mM EDTA] when necessary. MDS-L cells (28, 29) were kindly provided by Dr. Daniel Starczynowski (Cincinnati Children's Hospital Medical Center), and cultured in RPMI supplemented with 10% fetal bovine serum, penicillin/streptomycin and 10 ng/ml human IL-3 (hIL-3) (Peprotech). To induce the expression of shRNA and exogenous SRSF2 in MDS-L cell lines transduced with pTRIPZ vectors, 1 μg/ml Doxycycline (Sigma) was added every day to the cells for three days. To reach 50% SRSF2 expression in shRNA only cells, 2.5 μg/ml Doxycycline was used in the assay. Cell growth was evaluated in duplicate by the Trypan blue exclusion assay. As for colony forming unit (CFU) assays, specific numbers of cells (described in figure legends) were seeded into M3434 (STEMCELL Technologies). One week later, colony number was counted.

Flow cytometry

Primary cells from mice (FL, PB and BM cells) were treated with ACK buffer at room temperature for 5 minutes. For PB staining, B cell lineage (APC-conjugated B220), T cell lineage (PerCP-Cy5.5-conjugated CD4 and CD8a), or granuolocyte lineages (PE-conjugsted Gr1 and CD11b) were used. For FL staining, lineage cocktail was CD3, CD4, CD8a, Gr1, B220, CD19 and Ter119. For adult BM lineage cocktail, CD11b was added to that of FL. All of these antibodies are conjugated to PerCP-Cy5.5. Sca-1-APC, c-Kit-PECy7, CD48-PE and CD150-Biotin (all these antibodies from eBioscience) together with streptavidin-APC-Alexa Fluor 750 (Invitrogen) were used for SLAM staining. Data were collected on FACSCanto or FACSCalibur (both from BD), and analyzed by FACSDiva (BD) or FlowJo software (Treestar). For the apoptosis assay, Annexin V-APC apoptosis kit (BD) was used. Cell cycle was evaluated by Pyronin Y and 7AAD staining (30).

Reverse transcription (RT) and quantitative polymerase chain reaction (qPCR)

Total RNA was extracted by using Trizol (Life Technologies) and treated with DNase I (Qiagen). RT reactions were carried out by using the qScript cDNA Synthesis Kit (Quanta Biosciences). qPCR was performed with the SYBR FAST qPCR Kit (KAPA Biosystems). For validation of the results of RASL-seq, OneStep RT-PCR kit (Qiagen) was used. Primers used for RT-PCR and qPCR are as follows. mSrsf2(F): CGCGCTCCAGATCAACCTC. mSrsf2(R): CTTGGACTCTCGCTTCGACAC. mGAPDH(F): GGTGCTGAGTATGTCGTGGAGTCTA. mGAPDH(R): AAAGTTGTCATGGATGACCTTGG. hSRSF2 3'-UTR(F): GCACTAGGCGCAGTTGTGTA. hSRSF2 3'-UTR(R): CAATCGGGAGAAAACAGGAA. hSRSF2 Exon2 CDS(F): CTACAGCCGCTCGAAGTCTC. hSRSF2 Exon2 CDS(R): TTGGATTCCCTCTTGGACAC. hGAPDH(F): TCGCTCAGACACCATGGGGAAG. hGAPDH(R): GCCTTGACGGTGCCATGGAATTTG.

Western blotting

Cell extracts from mouse bone marrow were prepared with Thermo Scientific Pierce IP Lysis Buffer (PI-87787) including the protease inhibitor cocktail (PI-88665) and phosphatase inhibitor cocktail (PI-88667). Western blotting was performed following standard procedures. Protein samples were denatured in 1× loading buffer [10% glycerol, 2% SDS, 10 mM DTT and 50 mM Tris-HCl (pH 6.8)]. Protein concentration was adjusted and protein samples were loaded on SDS polyacrylamide gels after adding bromophenol blue (0.05%). Primary anti-SRSF2 antibody (ab28428; Abcam) and anti-β-actin antibody (A1978; Sigma-Aldrich) were used. Signals from fluorophore-conjugated secondary antibodies were detected with the Odyssey system (LI-COR).

Retrovirus infection

Virus infection procedure was performed as described previously (27). For general retrovirus infection, 293T cells were transfected with 5 μg of retrovirus vectors and with 5 μg of Ecopac packaging vector using polyethylenimine (Polysciences Inc). The 293T medium was changed from DMEM to IMDM 10 hrs post transfection. Retroviral supernatants were harvested 48 hrs after transfection and filtered through a 0.45 μm filter. The supernatant was added to primary bone marrow cells, along with 4% IL3-CM, 4%SCF-CM, 1% HEPES and 0.1% polybrene (final concentration 4 μg/mL). The cells were spinoculated at 1200 × *g* for 3 hrs at 32° C. Infections were performed twice on consecutive days. For overexpression of WT and mutant SRSF2, BM cells were transduced with MIP vector or MIP-SRSF2 expression retrovirus by two rounds of infection, selected in 1 μg/mL puromycin for 3 days before assays.

For lentivirus production, 293T cells were transfected with pTRIPZ lentivirus vectors, pCMV-VSVG, and pCMV-dR8.2 using lipofectamine 2000 (Life Technologies) for 6 hrs and then the medium was changed. Forty-eight hours later, culture supernatant was harvested, and filtered through a 0.45 μm filter. For viral transduction, RPMI1640 medium with 10 ng/ml hIL-3 was diluted with viral supernatant at 1:1 ratio. The MDS-L cells were then cultured in the mixed medium with 8 μg/ml polybrene overnight. Next day, medium was changed, and the stable cell lines with incorporated viral DNA segments were selected in 2 μg/ml puromycin for 7 days.

Stress hematopoiesis

5-FU (GeneraMedix) was injected *i.p.* every week (150 mg/kg body weight). Survival was monitored every day. The combined results of independent two experiments are shown.

For sublethal irradiation, mice received 4 Gy total body irradiation. Cell counts were followed up.

Bone marrow transplantation assay

For bone marrow transplantation (BMT) of Srsf2-overexpressed cells, donor C57BL/6 mice were injected *i.p.* with 150 mg/kg body weight 5-Fluorouracil (5-FU) five days prior to bone marrow harvest. BM cells were harvested, treated with ACK buffer, and washed with PBS. Cells were transduced with MigR1, MigR1-SRSF2^{WT}, and MigR1-SRSF2^{P95H} vectors. GFP percentage was adjusted to 17% using uninfected cells. Infected BM cells were injected into lethally irradiated recipient mice (9 Gy) through the tail veins. Recipient mice were given acidic water (pH 4.0) for three weeks following BMT.

For competitive and non-competitive BMT, total BM cells were harvested from indicated donor mice without treatment. In non-competitive settings, 2 million test cells in 200 μL PBS were injected into lethally irradiated (9 Gy) recipient PEP3 mice. In competitive settings, test cells were mixed with competitor cells (PEP3 cells) 1:1, and 2 million cells were injected into lethally irradiated recipient PEP3 mice.

RASL-seq

Doxycycline (Dox, Sigma) at indicated concentration was added to MDS-L cell culture every day for 3 days. Total RNA was extracted from cells, and used for RASL-seq. Analysis of splicing changes was described previously (25, 26). Gene function and pathway analyses were performed using QIAGEN's Ingenuity® Pathway Analysis (IPA®, QIAGEN Redwood City, www.qiagen.com/ingenuity). Original data is uploaded to GSE (GEO accession number: GSE61052).

Statistics

All the experiments were repeated at least twice. Results were represented as mean ± standard deviation (SD) unless otherwise stated. Comparison between two groups was done by t-test. Survival data were presented as Kaplan-Meyer curves, and Log-rank test was performed. $p < 0.05$ was considered as significant and shown by asterisk.

Results

Srsf2 is essential for viability of blood cells in vitro

To test the functional requirement of *Srsf2* in blood cells, we first pursued an in vitro model by infecting bone marrow (BM) cells derived from adult $Srsf2^{+/+}$ and $Srsf2^{f/f}$ mice with MSCV-Cre-IRES-EYFP (Cre) or empty vector (MSCV-IRES-EYFP) (EV) retrovirus. In the absence of Cre expression, $Srsf2^{+/+}$ (+/+ EV) and $Srsf2^{f/f}$ (f/f EV) cells did not show any growth difference. However, in the presence of Cre expression, $Srsf2^{f/f}$ cells (f/f Cre) exhibited a clear growth disadvantage compared to $Srsf2^{+/+}$ cells (+/+ Cre) (Figure 1A). In addition, Cre-infected $Srsf2^{f/f}$ (f/f Cre) cells were significantly more apoptotic compared to other groups (Figure 1B). These results demonstrate that Srsf2 is essential for blood cell growth and survival in vitro.

Srsf2 plays an indispensable role in the development of the hematopoietic system in mice

To pursue the functional impact of *Srsf2* deletion on hematopoietic cells under in vivo conditions, we first crossed $Srsf2^{f/f}$ mice with blood cell-specific Cre transgenic mice (*Vav-iCre*) (31). Fetal liver (FL) hematopoiesis was analyzed in multiple sets of littermates at embryonic day 12.5 and 14.5 (E12.5 and E14.5). Compared to others, *Vav-iCre*+$Srsf^{f/f}$ ($Srsf2^{\Delta/\Delta}$) embryos had paler and smaller FL (Figure 2A), which contained significantly fewer definitive blood cells (10% of wild type controls at E14.5) (Figure 2B). The remaining cells in $Srsf2^{\Delta/\Delta}$ FL exhibited more apoptosis and quiescence (Figure 2C-D), which is compatible with the in vitro data (Figure 1B). Histological study on E14.5 FLs showed that erythroblasts and mature granulocytes were not detectable in $Srsf2^{\Delta/\Delta}$ FLs (Figure 2E). $Srsf2^{\Delta/\Delta}$ embryos died during

embryonic development between E16.5-E18.5 with severe anemia and edema (Table 1 and data not shown). These results demonstrate the essential role of *Srsf2* in hematopoiesis during embryonic development.

To further characterize the defects in FL hematopoiesis, we next examined hematopoietic stem/progenitor cells (HSPCs) in FLs by flow cytometry. Importantly, we detected no HSPCs (lineage-/cKit+) in E14.5 $Srsf2^{\Delta/\Delta}$ FL hematopoietic cells (Figure 3A-B). In agreement with this result, a colony forming assay of E12.5 FL cells showed that $Srsf2^{\Delta/\Delta}$ cells had significantly lower clonogenicity (Figure 3C). Differential counts of colonies did not show significant changes between any groups (data not shown). In addition, peripheral blood (PB) of *Vav-iCre+*$Srsf2^{f/f}$ ($Srsf2^{\Delta/\Delta}$) embryos had significantly higher primitive red blood cells as shown by the number of nucleated erythrocytes (Figure 3D-E). Throughout these experiments, Δ/+ embryos did not show significant difference compared to +/+, suggesting that one allele is sufficient for normal HSC function. Thus, *Srsf2* is essential for the survival of embryonic HSPCs.

Srsf2 is required for survival of adult BM cells

Haploinsufficient expression of certain critical hematopoietic regulators, such as RUNX1 and PU.1, has been shown to affect both the number and distribution of different populations of blood cells (32, 33). Interestingly, most reported mutations of *SRSF2* in MDS are monoallelic, suggesting potential haploinsufficiency of *SRSF2* in disrupting hematopoiesis. To explore this possibility, we tested whether adult heterozygous mice (*Vav-iCre+*$Srsf2^{f/+}$, *Δ/+*) had recordable phenotypes relative to control mice (*Vav-iCre-*$Srsf2^{f/+}$, *f/+*). *Srsf2* expression, measured by RT-qPCR and western blot, was almost half in *Δ/+* BM cells compared to their *f/+* counterpart (data

not shown). We detected little difference between WT and heterozygous mice based on blood counts under either normal or stressed conditions [cell count recovery after sublethal irradiation (4 Gy) or weekly 5-FU injection (150 mg/kg), aging stress up to 10 months] (data not shown). These results suggest that SRSF2 level remains half in the heterozygous mice and its expression from one allele is sufficient for maintaining its normal cellular function.

Lack of SRSF2 in the developing heart resulted in dilated cardiomyopathy, while cKO of mature cardiomyocytes did not have any obvious phenotype (22, 23). These reports suggest that loss of SRSF2 can result in different phenotypes at different developmental stages. Therefore, we also evaluated the effect of SRSF2 ablation in adult blood cells. We crossed *Srsf2*$^{f/f}$ mice with *Mx1Cre* mice to generate polyinosinic:polycytidylic acid (polyIC)-inducible *Srsf2* knockout mice. Interestingly, *Mx1Cre+Srsf2*$^{f/f}$ mice stayed alive at least for 3 months after seven injections of 600 μg/dose polyIC (data not shown). Genotyping of blood and BM cells showed incomplete excision of the floxed *Srsf2* allele in blood and BM cells from *Mx1Cre+Srsf2*$^{f/f}$ mice. In contrast, we detected nearly complete ablation of the floxed allele in blood and BM cells from heterozygous *Mx1Cre+Srsf2*$^{f/+}$ mice (Figure 4A). Genotyping of colonies derived from single bone marrow cells confirmed incomplete knockout showing both floxed and deleted bands in *Mx1Cre+Srsf2*$^{f/f}$ cells (data not shown). These results indicate a high level of selection pressure against the loss of *Srsf2*. On day 16, polyIC-treated *Mx1Cre+Srsf2*$^{f/f}$ mice had significantly decreased platelet counts in their PB (Figure 4B). Other examined blood parameters, including neutrophil counts, percentage of myeloid (Gr1+/CD11b+), B (B220+), and T (CD4+/CD8+) cells were normal (data not shown). Decreased counts of white blood cells and lymphocytes in *Mx1Cre+Srsf2*$^{f/+}$ and *Mx1Cre+Srsf2*$^{f/f}$ mice were observed (data not shown), which is possibly due to Cre expression.

Importantly, BM showed a significant decrease in total BM cell counts, absolute number of Lineage-/Sca-1+/c-Kit+ (LSK) cells in total BM, and percent of LSK cells in BM of *Mx1Cre+Srsf2*$^{f/f}$ mice compared to *Mx1Cre-Srsf2*$^{f/f}$ controls (Figures 4C-E). SLAM staining using CD150 and CD48 antibodies did not record any significant change in the ratios of positive and negative cells (data not shown). These results suggest that the immature BM fraction (LSK) was more susceptible to the loss of SRSF2 compared to further differentiated cell populations.

To further establish that the observed phenotypes are cell-autonomous, we performed competitive bone marrow transplantation (BMT) of *Mx1Cre+Srsf2*$^{f/f}$ BM cells (Figure 4F). One month after BMT, *Mx1Cre+Srsf2*$^{f/f}$ recipients showed significantly lower engraftment even before polyIC injection, possibly due to high interferon sensitivity of *Mx1Cre+Srsf2*$^{f/f}$ cells induced early in the BMT procedure (34). PolyIC injection caused further decrease of donor chimerism in these mice. These results thus demonstrate the cell autonomous effect of *Srsf2* ablation on the survival of immature hematopoietic stem cells.

***Srsf2* overexpression also causes a growth disadvantage**

Single allele *SRSF2* mutations have been commonly identified in MDS patient (6, 16, 17, 19). On the other hand, heterozygous deletion of *Srsf2* in blood cells of *Vav-iCre+Srsf2*$^{f/+}$ (Figures 2-3) and polyIC -treated *Mx1Cre+Srsf2*$^{f/+}$ mice (Figures 4) did not show obvious phenotypes. These results suggest that *SRSF2* mutations in MDS are not simply loss-of-function mutations but rather reflect altered functions. We wished to further test the hypothesis of altered function under overexpression conditions, by selecting the MDS-associated P95H missense mutation and in-frame 8 amino-acid deletion (Δ8aa, P95 to R102 deletion) to

compare with WT SRSF2. MIP vector and MIP-WT, -P95H, and -△8aa *SRSF2* retroviruses were used to infect murine bone marrow cells. The exogenously expressed WT, P95H, and △8aa SRSF2 protein is 4-7 fold above the endogenous SRSF2 level (Figure 5A). Liquid culture of infected cells showed growth suppression by both WT and mutant SRSF2 under such overexpression conditions (Figure 5B). Importantly, the cells expressing the mutant *SRSF2* showed a significant increase in apoptosis relative to their WT counterpart (Figure 5C), though cell cycle was not inhibited (data not shown). Consistent with the liquid culture data, the colony forming assay showed significantly lower colony and cell numbers in WT-infected cells, which were even lower in P95H and Δ8aa cells compared to the MIP infected cells (Figure 5D). The colony types (GEMM, BFU-E, CFU-G, CFU-GM and CFU-GM), surface markers (Gr-1 and CD11b), and cell morphology were not different among the groups (data not shown). These results suggest that increased expression of SRSF2 mainly affects cell survival but does not disrupt myeloid cell differentiation. More importantly, overexpression of the P95H and Δ8aa mutants always showed stronger negative effects on cell survival than the WT SRSF2.

We next performed a transplantation of SRSF2 overexpressing bone marrow cells to evaluate the repopulation ability in vivo. The percentage of GFP+ cells in PB of WT- and P95H-cell recipients was lower than in MigR1-cell recipient mice. However, the difference between the WT and P95H groups was not significant (Figure 5E). Lineage staining of GFP+ PB cells did not show lineage skewing (myeloid vs lymphoid) in response to overexpression of WT or mutant SRSF2 (data not shown). Furthermore, these cells did not show a difference in dysplastic morphology in PB and BM during the observation of 10 months (data not shown). Data in these experiments suggest that overexpressed WT and P95H both caused significant

growth disadvantage, which was also accompanied by induced apoptosis. However, neither appears to have any recordable effect on cell differentiation both in vitro and in vivo.

SRSF2 Mutants altered a large RNA splicing program

Although our functional analysis of overexpressed SRSF2 is consistent with earlier reports of overexpressed SR proteins interfering with developmental processes (35-37), the data indicate a clear advantage in studying the mutant function of SRSF2 in cellular systems that may enable us to recapitulate *SRSF2* single allele mutations in MDS patients. We generated a relatively low-level expression system by lowering endogenous *SRSF2* with shRNA and simultaneously expressing the mutant version of the protein in a human MDS cell line (MDS-L) (28, 29). This cell line was derived from an MDS patient and has a chromosome 5q deletion but no mutation in splicing factors *SRSF2* or *U2AF1* (confirmed by re-sequencing, data not shown). We constructed Tet-inducible lentivirus vectors to co-express an shRNA targeting the 3'-UTR of endogenous *SRSF2* and an shRNA-resistant form of *SRSF2* cDNA (WT or mutants) (Figure 6A). MDS-L cells were transduced with *SRSF2* shRNA/cDNA lentivirus to establish pools of shRNA/*WT*, *P95H*, and *⊿8aa* inducible expressing cells. Doxycycline (Dox) treatment reduced endogenous SRSF2 (shown by 3'-UTR expression) while inducing relatively low overexpression of total *SRSF2* RNA (3 to 4 fold of the endogenous level) [shown by exon 2 coding sequence (CDS)] (Figure 6B). Under these conditions, mutant cells (P95H and Δ8aa) showed significant growth arrest and enhanced apoptosis compared to WT cells (Figure 6C-D). However, cell cycle analysis did not show any obvious change except for a detectable increase in sub-G0/G1 cells (data not shown). These

data indicate that the system closely mimics certain MDS conditions in a disease-relevant cell line.

Although it is widely anticipated that *SRSF2* mutations will perturb the splicing program in diseased cells, the global impact of *SRSF2* mutations on regulated splicing has not been investigated. To reveal potential functional differences between WT and mutant SRSF2 that may be relevant to MDS development, we examined the splicing response by using the RASL-seq platform, which was designed to detect annotated 5530 alternatively spliced mRNA isoforms in the human genome (26). MDS-L cells co-expressing Tet-inducible *SRSF2* shRNA and WT, P95H, or Δ8aa SRSF2 were cultured with or without Dox for 3 days to modulate SRSF2 expression. Total RNA was isolated from these cells for splicing profiling.

Based on a stringent cutoff (a fold ratio change >1.5 and p-value<0.05), we detected both overlapped and separated changes in splicing upon expression of WT and mutant SRSF2 (Figure 7A-B, Table S1-5), indicating that MDS-associated mutations have a shared function with and an independent effect from WT SRSF2 on splicing. Relative to WT cells, P95H and ∆8aa mutants induced a common set of 487 events, 470 of which were altered in the same directions, including 164 enhanced cassette exon inclusion and 306 enhanced cassette exon exclusion (Figure 7C, Table S6). Importantly, P95H and ∆8aa mutants each induced 210 and 483 extra events, respectively. Ten commonly changed splicing events in genes related to hematopoiesis was selected and validated by RT-PCR (Figure 7D). Similar to shSRSF2 only, MEIS1, UPF38 and PRKAA1 had increased ratios of short to long isoforms in SRSF2 mutant cells, suggesting reduction of SRSF2 function of SRSF2 mutants in these splicing events. RBM23, PDK1, PDE4DIP, MLL and RNF34 had increased while CBFB and SMG7 had decreased short to long isoform ratios in SRSF2 mutant cells independent of shSRSF2,

suggesting the gain of function effect of SRSF2 P95H and Δ8aa mutants in these splicing events. Furthermore, the change of the scale of exon inclusion or exclusion induced by Δ8aa mutant is over 1.5 times more in 450 out of 470 common events relative to the P95H mutant. Together, these data suggest that even though the two mutants showed certain overlapping effects on splicing, they were not functionally equivalent; the deletion mutant may have a more profound impact on regulated splicing than the P95H mutation.

To gain functional insights into such a dramatically altered splicing program, we reasoned that the altered splice events commonly affected by P95H and Δ8aa might be more related to MDS, while extra events induced by each mutant might be responsible for enhancing the disease phenotype. We thus focused on the commonly affected set of 470 genes by applying Ingenuity pathway analysis. Consistent with the functional consequences triggered by the mutations in our cellular and animal models, we observed cancer development and apoptosis pathways among the top 10-ranked canonical pathways (Figure 8A). These findings support the possibility that the MDS-associated mutations in *SRSF2* promote the development of the disease phenotype with potential to induce a cascade of events that lead to both disease progression and more aggressive types of blood disorders.

To analyze the possible loss or gain of function of the P95H and Δ8aa mutations, we also examined their 470 commonly affected splicing events in MDS-L cells that expressed only shRNA of *SRSF2* but not any shRNA resistant *SRSF2*. Upon Dox treatment, SRSF2 expression in these cells was knocked down nearly 50% (data not shown). One hundred thirty-five events (29% of 470) were affected by the SRSF2 reduction (Figure 8B, Table S7). Interestingly, we detected similar numbers of splicing events changed in the same and the opposite directions between the SRSF2 mutants and knockdown cells. The remaining 335 of

470 events were not affected by *SRSF2* knockdown. These results suggest that P95H and Δ8aa mutations lead to loss of function in some splicing events (shared and in the same direction), enhanced function in some other WT SRSF2 involved splicing events (shared but in the opposite direction), and also potentially gain of function in regulating new splicing events (not overlapped). It is possible that some of these combinatory loss and gain effects promote MDS development.

Discussion

In this report, we examined the role of SRSF2 in hematopoiesis using the *Srsf2* cKO mouse model. We also analyzed the cellular effect of expressing MDS-related mutant forms of SRSF2. Our analyses demonstrate that SRSF2 is essential for the survival of blood cells including HSCs. In the absence of SRSF2, blood cells had increased senescence and apoptosis. However, unlike previous reports in several other cellular systems, we did not detect any significant delay of cell cycle in SRSF2-deficient blood cells, nor observed the effect on differentiation of myeloid cells. Interestingly, ablation of SRSF2 in pituitary cells and thymocytes results in decreased organ size but no increase of apoptosis (23, 24). Developing thymocytes showed a differentiation block from CD4/CD8 double negative to double positive stage (24). Ablation of SRSF2 in the embryonic heart showed normal development but later suffered from dilated cardiomyopathy (22). However, mice with *Srsf2* knockout in post-mitotic cardiomyocytes stayed normal (23). These different phenotypes of SRSF2 in different cell types may result from alteration of cell type-specific targets of SRSF2. For example, in thymocytes lacking SRSF2, the defective splicing of lymphoid cell-specific CD45 RNA has been related to their abnormal differentiation (23).

SR proteins including SRSF2 are known to autoregulate their own expression via an intron retention event in its 3'-UTR (38-40). In response to SRSF2 overexpression, splicing of this retained intron likely produces an exon junction complex (EJC), triggering nonsense-mediated mRNA decay. As the intron is mostly retained in normal cells, reduction of SRSF2 may have little effect on mRNA stability. Consistently, we detected nearly a 50% decrease of SRSF2 in $Srsf2^{\Delta/+}$ heterozygous blood cells. In light of a recent report that heterozygous *Sf3b1*

deficient mice showed haploinsufficiency in HSCs (41) and because *SRSF2* mutations in MDS patients are generally heterozygous, we examined hematopoiesis in mice with *Srsf2* heterozygous blood cells during development and under stress conditions. No obvious phenotypes were observed, suggesting that the MDS-related heterozygous *SRSF2* mutations are not simply loss-of-function mutations and that MDS may not result from *SRSF2* haploinsufficiency. Instead, our data suggest likely gain-of-function mutations in *SRSF2*, including potential dominant negative effects that reduce total SRSF2 activity.

It is striking that *SRSF2* mutations in MDS mainly occur at proline 95 (P95), suggesting a critical role of P95 in SRSF2. SRSF2 has an N-terminal RNA recognition (RRM) domain and a C-terminal arginine and serine rich (RS) domain. The RRM domain is primarily involved in specific RNA recognition. The RS domain can be highly phosphorylated and is involved in both RNA binding and protein-protein interactions during spliceosome assembly (21). P95 is generally believed to be located in the hinge region between the RRM domain and the RS domain. A recent structural analysis of the N-terminal 101 amino acids of SRSF2 bound to 6-oligonucleotide RNA targets showed that P95 directly contacts the C3 and G3 nucleotides in RNA containing the UCCAGU and UGGAGU motifs, which represent two consensus SRSF2 binding sequences (42). It is possible that SRSF2 with mutations at P95 decrease the RNA binding specificity. This possibility is supported by a recent report that unlike the WT SRSF2, the P95H mutant preferentially binds to CCAG motif (43). Furthermore, the unique features of proline among the 20 protein-forming amino acids, including its cis-trans isomerization (44), CH/Pi hydrogen bond formation (45), and higher conformational rigidity in the secondary structure of proteins (44), may result in a different local structure to create a new surface for

441 interaction with additional proteins and RNA sequences. These are subject to future
442 biochemical studies.

443 We compared WT and mutant (P95H, and Δ8aa) SRSF2 by overexpressing them via
444 MSCV retrovirus transduction. With this approach, exogenously expressed SRSF2 protein is 4
445 to 7 fold above its endogenous level. Similar inhibitory effects of WT and both mutants on cell
446 growth, colony formation, and in vivo blood cell repopulation were detected in these
447 overexpression assays (Figure 5). These results support the above hypothesis that WT and
448 P95 mutant SRSF2 have certain similar functions, and such functions above normal levels
449 disrupt hematopoiesis. Interestingly, the negative effects of over expressing the WT SRSF2
450 and P95H are nearly identical on in vivo repopulation (Figure 5D), suggesting that HSPCs are
451 likely more sensitive to the level of SRSF2.

452 We also used the Tet-On system to induce co-expression of an *SRSF2* shRNA and an
453 shRNA-resistant WT or mutant *SRSF2* to mimic patient expression levels in the MDS-L cell
454 line. Under this experimental setting, we detected unique cell growth inhibitory effects of
455 mutant *SRSF2*, which is more likely due to the unique gain/loss functions of mutant *SRSF2*.

456 Using the RASL-seq platform, we observed that apoptosis and cancer-related pathways
457 were among the top 10 ranked canonical pathways affected by SRSF2 mutations, which is
458 consistent with pathology of MDS patient cells (1, 2). MDS cells were noted to be highly
459 apoptotic at early stages, likely reflecting a key mechanism to eliminate cells and eventually
460 become malignant (1, 2, 46). Thus, mutant forms of *SRSF2* in MDS seem to trigger genomic
461 instability, and promote accumulation of unwanted oncogenic mutations (47). RASL-seq (25,
462 26) is a convenient way to screen the alternative splicing changes with multiple advantages,
463 including (1) the ability to use limited amounts of total RNA for the analysis (typically from 0.1

to 1 μg of total RNA), (2) considerable tolerance of RNA quality to obtain robust data, (3) the sensitivity to obtain quantitative information on alternative splicing events in less abundant transcripts, and (4) the ability for highly parallel analyses of biological samples in a cost-effective manner. However, compared to RNA-seq, RASL-seq is limited to analysis of annotated alternative splicing events and cannot detect other aberrant RNA processing events. Despite these limitations, we successfully applied this technique to identify a large cohort of alternative splicing events uniquely caused by mutant *SRSF2*, suggesting that the mutant splicing factor has the capacity to dramatically alter the splicing program in diseased cells. It is unclear whether the mutant *Srsf2* also affects certain constitutive splicing events.

In conclusion, we demonstrate that SRSF2 is essential for the survival of hematopoietic cells and that its loss results in apoptosis and growth suppression. No obvious phenotypes were detected in *Srsf2* heterozygous blood cells, but growth arrest and increased apoptosis were clearly detected in cells expressing either P95H or Δ8aa mutants. Together, these results support that MDS-related *SRSF2* mutations are not simply loss-of-function mutations. Furthermore, RASL-seq analysis demonstrates that MDS mutant forms of SRSF2 dysregulate RNA splicing. Future work will be focused on understanding the molecular mechanism of *SRSF2* mutations in MDS development, including their effects on RNA splicing and other aspects of regulated gene transcription (48, 49). Future studies will also examine how mutations in *SRSF2* may act in synergy with mutations in other key leukemia genes, such as TET2, IDH2, and RUNX1, to propel MDS progression to more aggressive blood cell disorders.

Acknowledgments

This work was supported by NIHR01DK098808. YK was supported partially by Sumitomo Life Social Welfare Services Foundation and Mochida Memorial Foundation for Medical and Pharmaceutical Research. YJH is supported partially by a scholarship from Ministry of Education from the Republic of China. We thank Amanda Scholl for editing the manuscript, Dr. Omar Abdel-Wahab for critical review, Dr. Daniel Starczynowski (for providing MDS-L cells, and Dr. Gregory Hannon for providing pTRIPZ vector.

References

1. **Ades L, Itzykson R, Fenaux P.** 2014. Myelodysplastic syndromes. Lancet doi:10.1016/S0140-6736(13)61901-7.

2. **Malcovati L, Hellstrom-Lindberg E, Bowen D, Ades L, Cermak J, Del Canizo C, Della Porta MG, Fenaux P, Gattermann N, Germing U, Jansen JH, Mittelman M, Mufti G, Platzbecker U, Sanz GF, Selleslag D, Skov-Holm M, Stauder R, Symeonidis A, van de Loosdrecht AA, de Witte T, Cazzola M.** 2013. Diagnosis and treatment of primary myelodysplastic syndromes in adults: recommendations from the European LeukemiaNet. Blood **122:**2943-2964.

3. **Kulasekararaj AG, Mohamedali AM, Mufti GJ.** 2013. Recent advances in understanding the molecular pathogenesis of myelodysplastic syndromes. Br J Haematol **162:**587-605.

4. **Walter MJ, Shen D, Shao J, Ding L, White BS, Kandoth C, Miller CA, Niu B, McLellan MD, Dees ND, Fulton R, Elliot K, Heath S, Grillot M, Westervelt P, Link DC, DiPersio JF, Mardis E, Ley TJ, Wilson RK, Graubert TA.** 2013. Clonal diversity of recurrently mutated genes in myelodysplastic syndromes. Leukemia **27:**1275-1282.

5. **Bejar R, Stevenson K, Abdel-Wahab O, Galili N, Nilsson B, Garcia-Manero G, Kantarjian H, Raza A, Levine RL, Neuberg D, Ebert BL.** 2011. Clinical effect of point mutations in myelodysplastic syndromes. N Engl J Med **364:**2496-2506.

6. **Yoshida K, Sanada M, Shiraishi Y, Nowak D, Nagata Y, Yamamoto R, Sato Y, Sato-Otsubo A, Kon A, Nagasaki M, Chalkidis G, Suzuki Y, Shiosaka M, Kawahata R, Yamaguchi T, Otsu M, Obara N, Sakata-Yanagimoto M, Ishiyama K, Mori H, Nolte F, Hofmann WK, Miyawaki S, Sugano S, Haferlach C, Koeffler HP, Shih LY, Haferlach T, Chiba S, Nakauchi H, Miyano S, Ogawa S.** 2011. Frequent pathway mutations of splicing machinery in myelodysplasia. Nature **478:**64-69.

7. **Graubert TA, Shen D, Ding L, Okeyo-Owuor T, Lunn CL, Shao J, Krysiak K, Harris CC, Koboldt DC, Larson DE, McLellan MD, Dooling DJ, Abbott RM, Fulton RS, Schmidt H, Kalicki-Veizer J, O'Laughlin M, Grillot M, Baty J, Heath S, Frater JL, Nasim T, Link DC, Tomasson MH, Westervelt P, DiPersio JF, Mardis ER, Ley TJ, Wilson RK, Walter MJ.** 2012. Recurrent mutations in the U2AF1 splicing factor in myelodysplastic syndromes. Nat Genet **44:**53-57.

8. **Yoshida K, Ogawa S.** 2014. Splicing factor mutations and cancer. Wiley Interdiscip Rev RNA **5:**445-459.

9. **Papaemmanuil E, Cazzola M, Boultwood J, Malcovati L, Vyas P, Bowen D, Pellagatti A, Wainscoat JS, Hellstrom-Lindberg E, Gambacorti-Passerini C, Godfrey AL, Rapado I, Cvejic A, Rance R, McGee C, Ellis P, Mudie LJ, Stephens**

PJ, McLaren S, Massie CE, Tarpey PS, Varela I, Nik-Zainal S, Davies HR, Shlien A, Jones D, Raine K, Hinton J, Butler AP, Teague JW, Baxter EJ, Score J, Galli A, Della Porta MG, Travaglino E, Groves M, Tauro S, Munshi NC, Anderson KC, El-Naggar A, Fischer A, Mustonen V, Warren AJ, Cross NC, Green AR, Futreal PA, Stratton MR, Campbell PJ. 2011. Somatic SF3B1 mutation in myelodysplasia with ring sideroblasts. N Engl J Med **365:**1384-1395.

10. **Visconte V, Makishima H, Jankowska A, Szpurka H, Traina F, Jerez A, O'Keefe C, Rogers HJ, Sekeres MA, Maciejewski JP, Tiu RV.** 2012. SF3B1, a splicing factor is frequently mutated in refractory anemia with ring sideroblasts. Leukemia **26:**542-545.

11. **Zhang SJ, Rampal R, Manshouri T, Patel J, Mensah N, Kayserian A, Hricik T, Heguy A, Hedvat C, Gonen M, Kantarjian H, Levine RL, Abdel-Wahab O, Verstovsek S.** 2012. Genetic analysis of patients with leukemic transformation of myeloproliferative neoplasms shows recurrent SRSF2 mutations that are associated with adverse outcome. Blood **119:**4480-4485.

12. **Damm F, Nguyen-Khac F, Fontenay M, Bernard OA.** 2012. Spliceosome and other novel mutations in chronic lymphocytic leukemia and myeloid malignancies. Leukemia **26:**2027-2031.

13. **Quesada V, Conde L, Villamor N, Ordonez GR, Jares P, Bassaganyas L, Ramsay AJ, Bea S, Pinyol M, Martinez-Trillos A, Lopez-Guerra M, Colomer D, Navarro A, Baumann T, Aymerich M, Rozman M, Delgado J, Gine E, Hernandez JM, Gonzalez-Diaz M, Puente DA, Velasco G, Freije JM, Tubio JM, Royo R, Gelpi JL, Orozco M, Pisano DG, Zamora J, Vazquez M, Valencia A, Himmelbauer H, Bayes M, Heath S, Gut M, Gut I, Estivill X, Lopez-Guillermo A, Puente XS, Campo E, Lopez-Otin C.** 2012. Exome sequencing identifies recurrent mutations of the splicing factor SF3B1 gene in chronic lymphocytic leukemia. Nat Genet **44:**47-52.

14. **Rossi D, Bruscaggin A, Spina V, Rasi S, Khiabanian H, Messina M, Fangazio M, Vaisitti T, Monti S, Chiaretti S, Guarini A, Del Giudice I, Cerri M, Cresta S, Deambrogi C, Gargiulo E, Gattei V, Forconi F, Bertoni F, Deaglio S, Rabadan R, Pasqualucci L, Foa R, Dalla-Favera R, Gaidano G.** 2011. Mutations of the SF3B1 splicing factor in chronic lymphocytic leukemia: association with progression and fludarabine-refractoriness. Blood **118:**6904-6908.

15. **Dolnik A, Engelmann JC, Scharfenberger-Schmeer M, Mauch J, Kelkenberg-Schade S, Haldemann B, Fries T, Kronke J, Kuhn MW, Paschka P, Kayser S, Wolf S, Gaidzik VI, Schlenk RF, Rucker FG, Dohner H, Lottaz C, Dohner K, Bullinger L.** 2012. Commonly altered genomic regions in acute myeloid leukemia are enriched for somatic mutations involved in chromatin remodeling and splicing. Blood **120:**e83-92.

16. **Thol F, Kade S, Schlarmann C, Loffeld P, Morgan M, Krauter J, Wlodarski MW, Kolking B, Wichmann M, Gorlich K, Gohring G, Bug G, Ottmann O, Niemeyer CM, Hofmann WK, Schlegelberger B, Ganser A, Heuser M.** 2012. Frequency and

prognostic impact of mutations in SRSF2, U2AF1, and ZRSR2 in patients with myelodysplastic syndromes. Blood **119:**3578-3584.

17. **Papaemmanuil E, Gerstung M, Malcovati L, Tauro S, Gundem G, Van Loo P, Yoon CJ, Ellis P, Wedge DC, Pellagatti A, Shlien A, Groves MJ, Forbes SA, Raine K, Hinton J, Mudie LJ, McLaren S, Hardy C, Latimer C, Della Porta MG, O'Meara S, Ambaglio I, Galli A, Butler AP, Walldin G, Teague JW, Quek L, Sternberg A, Gambacorti-Passerini C, Cross NC, Green AR, Boultwood J, Vyas P, Hellstrom-Lindberg E, Bowen D, Cazzola M, Stratton MR, Campbell PJ.** 2013. Clinical and biological implications of driver mutations in myelodysplastic syndromes. Blood **122:**3616-3627; quiz 3699.

18. **Hirabayashi S, Flotho C, Moetter J, Heuser M, Hasle H, Gruhn B, Klingebiel T, Thol F, Schlegelberger B, Baumann I, Strahm B, Stary J, Locatelli F, Zecca M, Bergstraesser E, Dworzak M, van den Heuvel-Eibrink MM, De Moerloose B, Ogawa S, Niemeyer CM, Wlodarski MW.** 2012. Spliceosomal gene aberrations are rare, coexist with oncogenic mutations, and are unlikely to exert a driver effect in childhood MDS and JMML. Blood **119:**e96-99.

19. **Makishima H, Visconte V, Sakaguchi H, Jankowska AM, Abu Kar S, Jerez A, Przychodzen B, Bupathi M, Guinta K, Afable MG, Sekeres MA, Padgett RA, Tiu RV, Maciejewski JP.** 2012. Mutations in the spliceosome machinery, a novel and ubiquitous pathway in leukemogenesis. Blood **119:**3203-3210.

20. **Wu SJ, Kuo YY, Hou HA, Li LY, Tseng MH, Huang CF, Lee FY, Liu MC, Liu CW, Lin CT, Chen CY, Chou WC, Yao M, Huang SY, Ko BS, Tang JL, Tsay W, Tien HF.** 2012. The clinical implication of SRSF2 mutation in patients with myelodysplastic syndrome and its stability during disease evolution. Blood **120:**3106-3111.

21. **Zhou Z, Fu XD.** 2013. Regulation of splicing by SR proteins and SR protein-specific kinases. Chromosoma **122:**191-207.

22. **Ding JH, Xu X, Yang D, Chu PH, Dalton ND, Ye Z, Yeakley JM, Cheng H, Xiao RP, Ross J, Chen J, Fu XD.** 2004. Dilated cardiomyopathy caused by tissue-specific ablation of SC35 in the heart. EMBO J **23:**885-896.

23. **Xiao R, Sun Y, Ding JH, Lin S, Rose DW, Rosenfeld MG, Fu XD, Li X.** 2007. Splicing regulator SC35 is essential for genomic stability and cell proliferation during mammalian organogenesis. Mol Cell Biol **27:**5393-5402.

24. **Wang HY, Xu X, Ding JH, Bermingham JR, Jr., Fu XD.** 2001. SC35 plays a role in T cell development and alternative splicing of CD45. Mol Cell **7:**331-342.

25. **Li H, Qiu J, Fu XD.** 2012. RASL-seq for massively parallel and quantitative analysis of gene expression. Curr Protoc Mol Biol **Chapter 4:**Unit 4 13 11-19.

26. **Zhou Z, Qiu J, Liu W, Zhou Y, Plocinik RM, Li H, Hu Q, Ghosh G, Adams JA, Rosenfeld MG, Fu XD.** 2012. The Akt-SRPK-SR axis constitutes a major pathway in transducing EGF signaling to regulate alternative splicing in the nucleus. Mol Cell **47:**422-433.

27. **Komeno Y, Yan M, Matsuura S, Lam K, Lo MC, Huang YJ, Tenen DG, Downing JR, Zhang DE.** 2014. Runx1 exon 6 related alternative splicing isoforms differentially regulate hematopoiesis in mice. Blood doi:10.1182/blood-2013-08-521252.

28. **Matsuoka A, Tochigi A, Kishimoto M, Nakahara T, Kondo T, Tsujioka T, Tasaka T, Tohyama Y, Tohyama K.** 2010. Lenalidomide induces cell death in an MDS-derived cell line with deletion of chromosome 5q by inhibition of cytokinesis. Leukemia **24:**748-755.

29. **Drexler HG, Dirks WG, Macleod RA.** 2009. Many are called MDS cell lines: one is chosen. Leuk Res **33:**1011-1016.

30. **Toba K, Winton EF, Koike T, Shibata A.** 1995. Simultaneous three-color analysis of the surface phenotype and DNA-RNA quantitation using 7-amino-actinomycin D and pyronin Y. J Immunol Methods **182:**193-207.

31. **de Boer J, Williams A, Skavdis G, Harker N, Coles M, Tolaini M, Norton T, Williams K, Roderick K, Potocnik AJ, Kioussis D.** 2003. Transgenic mice with hematopoietic and lymphoid specific expression of Cre. Eur J Immunol **33:**314-325.

32. **Iwasaki H, Somoza C, Shigematsu H, Duprez EA, Iwasaki-Arai J, Mizuno S, Arinobu Y, Geary K, Zhang P, Dayaram T, Fenyus ML, Elf S, Chan S, Kastner P, Huettner CS, Murray R, Tenen DG, Akashi K.** 2005. Distinctive and indispensable roles of PU.1 in maintenance of hematopoietic stem cells and their differentiation. Blood **106:**1590-1600.

33. **Sun W, Downing JR.** 2004. Haploinsufficiency of AML1 results in a decrease in the number of LTR-HSCs while simultaneously inducing an increase in more mature progenitors. Blood **104:**3565-3572.

34. **Cong X, Yan M, Yin X, Zhang DE.** 2010. Hematopoietic cells from Ube1L-deficient mice exhibit an impaired proliferation defect under the stress of bone marrow transplantation. Blood Cells Mol Dis **45:**103-111.

35. **Lopato S, Kalyna M, Dorner S, Kobayashi R, Krainer AR, Barta A.** 1999. atSRp30, one of two SF2/ASF-like proteins from Arabidopsis thaliana, regulates splicing of specific plant genes. Genes Dev **13:**987-1001.

36. **Kraus ME, Lis JT.** 1994. The concentration of B52, an essential splicing factor and regulator of splice site choice in vitro, is critical for Drosophila development. Mol Cell Biol **14:**5360-5370.

37. **Labourier E, Bourbon HM, Gallouzi IE, Fostier M, Allemand E, Tazi J.** 1999. Antagonism between RSF1 and SR proteins for both splice-site recognition in vitro and Drosophila development. Genes Dev **13:**740-753.

38. **Sureau A, Gattoni R, Dooghe Y, Stevenin J, Soret J.** 2001. SC35 autoregulates its expression by promoting splicing events that destabilize its mRNAs. EMBO J **20:**1785-1796.

39. **Lareau LF, Inada M, Green RE, Wengrod JC, Brenner SE.** 2007. Unproductive splicing of SR genes associated with highly conserved and ultraconserved DNA elements. Nature **446:**926-929.

40. **Ni JZ, Grate L, Donohue JP, Preston C, Nobida N, O'Brien G, Shiue L, Clark TA, Blume JE, Ares M, Jr.** 2007. Ultraconserved elements are associated with homeostatic control of splicing regulators by alternative splicing and nonsense-mediated decay. Genes Dev **21:**708-718.

41. **Matsunawa M, Yamamoto R, Sanada M, Sato-Otsubo A, Shiozawa Y, Yoshida K, Otsu M, Shiraishi Y, Miyano S, Isono K, Koseki H, Nakauchi H, Ogawa S.** 2014. Haploinsufficiency of Sf3b1 leads to compromised stem cell function but not to myelodysplasia. Leukemia doi:10.1038/leu.2014.73.

42. **Daubner GM, Clery A, Jayne S, Stevenin J, Allain FH.** 2012. A syn-anti conformational difference allows SRSF2 to recognize guanines and cytosines equally well. EMBO J **31:**162-174.

43. **Kim E, Ilagan JO, Liang Y, Daubner GM, Lee SC, Ramakrishnan A, Li Y, Chung YR, Micol JB, Murphy ME, Cho H, Kim MK, Zebari AS, Aumann S, Park CY, Buonamici S, Smith PG, Deeg HJ, Lobry C, Aifantis I, Modis Y, Allain FH, Halene S, Bradley RK, Abdel-Wahab O.** 2015. SRSF2 Mutations Contribute to Myelodysplasia by Mutant-Specific Effects on Exon Recognition. Cancer Cell **27:**617-630.

44. **MacArthur MW, Thornton JM.** 1991. Influence of proline residues on protein conformation. J Mol Biol **218:**397-412.

45. **Ozawa T, Okazaki K, Kitaura K.** 2011. Importance of CH/pi hydrogen bonds in recognition of the core motif in proline-recognition domains: an ab initio fragment molecular orbital study. J Comput Chem **32:**2774-2782.

46. **Zhou T, Hasty P, Walter CA, Bishop AJ, Scott LM, Rebel VI.** 2013. Myelodysplastic syndrome: an inability to appropriately respond to damaged DNA? Exp Hematol **41:**665-674.

47. **Montecucco A, Biamonti G.** 2013. Pre-mRNA processing factors meet the DNA damage response. Front Genet **4:**102.

48. **Ji X, Zhou Y, Pandit S, Huang J, Li H, Lin CY, Xiao R, Burge CB, Fu XD.** 2013. SR proteins collaborate with 7SK and promoter-associated nascent RNA to release paused polymerase. Cell **153:**855-868.

49. **Mo S, Ji X, Fu XD.** 2013. Unique role of SRSF2 in transcription activation and diverse functions of the SR and hnRNP proteins in gene expression regulation. Transcription **4:**251-259.

680 **Table 1. Number of surviving and dead mice with different genotypes of *Srsf2*.**

Day	Genotype			
	f/+	f/f	Δ/+	Δ/Δ
E11.5	4	2	1	3
E12.5	5	2	1	0
E13.5	3	3	1	0
E14.5	3	3	4	5
E15.5	2	1	1	2
E16.5	3	2	4	Alive 2
				Dead 4
E17.5	5	5	6	Alive 0
				Dead 3
E18.5	3	5	2	Alive 0
				Dead 6
P21	7	4	6	0

681 f/+, *Srsf2*$^{f/+}$. f/f, *Srsf2*$^{f/f}$. Δ/+, *Srsf2*$^{\Delta/+}$. Δ/Δ, *Srsf2*$^{\Delta/\Delta}$. E, embryonic day. P, postnatal day.

682 **Figure Legends**

683

684 **Figure 1. SRSF2 is essential for survival of adult BM cells in vitro.** (A) MSCV-IRES-EYFP
685 empty vector (EV) or MSCV-Cre-IRES-EYFP (Cre) retrovirus-infected *Srsf2* +/+ and f/f cells
686 were seeded in duplicate, and cell number was counted with Trypan blue staining. The number
687 of retrovirus-infected cells was determined based on EYFP expression. Cre-expressing *Srsf2*
688 cKO cells (f/f Cre) showed growth suppression. (B) Apoptosis of EYFP+ cells on day 3. EYFP+
689 cells were gated and early apoptotic cells were defined as AnnexinV+ 7AAD- cells. Cre+*Srsf2*
690 f/f cells showed significantly enhanced apoptosis. Results of three independent experiments
691 were used for statistical calculations. * indicates $p < 0.05$; ** indicates $p < 0.005$.

692

693 **Figure 2. Fetal liver (FL) hematopoiesis is defective in *Vav-iCre+Srsf2$^{f/f}$* embryos.** *Vav-*
694 *iCre+/ Srsf2$^{f/+}$* mice were crossed with *Srsf2$^{f/f}$* mice to generate *Vav-iCre-Srsf2$^{f/+}$* (f/+), *Vav-*
695 *iCre+Srsf2$^{f/+}$* (Δ/+), *Vav-iCre-Srsf2$^{f/f}$* (f/f), and *Vav-iCre+/Srsf2$^{f/f}$* (Δ/Δ) embryos. (A)
696 Macroscopic appearance of E12.5 and E14.5 embryos. *Srsf2$^{\Delta/\Delta}$* have smaller FLs compared
697 with the controls. (B) Relative cell numbers of E14.5 fetal livers. Each cell number was
698 normalized to the average of f/+ FLs in the same litter. Horizontal bars show the average of
699 each group. f/+, n = 4; f/f, n = 7; Δ/+, n = 6; Δ/Δ, n = 7. *Srsf2$^{\Delta/\Delta}$* FL cells were significantly
700 fewer than those in other groups. (C) Apoptosis assay. Early apoptotic cells were defined as
701 AnnexinV+ 7AAD- cells. f/+, n = 5; f/f, n = 2, Δ/+, n = 6; and Δ/Δ, n = 6. *Srsf2$^{\Delta/\Delta}$* FLs had
702 significantly more apoptotic cells than those in other groups. (D) Cell cycle analysis by Pyronin
703 Y and 7AAD staining. *Srsf2$^{\Delta/\Delta}$* FL cells show both a significant increase in apoptotic (sub-
704 G0/G1) cells and a decrease in cycling (S/G2/M) cells compared to other groups. f/+, n = 5; f/f,

n = 2; Δ/+, n = 6; and Δ/Δ, n = 6. (E) Histology of E14.5 FL (Hematoxylin-Eosin stain). *Srsf2*$^{\Delta/\Delta}$ FL consists of hepatoblasts characterized by a large, pale-staining nucleus with distinct nucleoli (arrowhead). FLs of other genotypes are filled with hematopoietic cells, the majority of which are erythroblasts (black arrow), with scattered white blood cells (white arrow). Original magnification, ×200. Insets, ×400. Objective lens, UPlanFL N 20×/0.50, UPlanFL N 40×/0.75 (both from Olympus, Tokyo). Images were acquired at room temperature using Olympus BX51 microscope equipped with DP71 camera and DP controller/DP Manager software (Olympus, Tokyo, Japan). * indicates $p < 0.05$; ** indicates $p < 0.005$.

Figure 3. *Srsf2* null fetal livers lack hematopoietic stem/progenitor cells. (A) Representative flow cytometry results of E14.5 FL cells. Lin-neg, lineage-negative. *Srsf2*$^{\Delta/\Delta}$ FL lacked Lin-neg/c-Kit+ (LK) and Lin-neg/Sca1+/c-Kit+ (LSK) cells. (B) Quantification of panel A. f/+, n = 10; f/f, n = 12; Δ/+, n = 5; and Δ/Δ, n = 6. (C) Colony formation assay of E12.5 FL cells. Cells (2×10^4) were seeded in duplicate. f/+, n = 8; f/f, n = 24; Δ/+, n = 10; and Δ/Δ, n = 6. *Srsf2*$^{\Delta/\Delta}$ FL cells showed significantly lower colony-forming ability than others. (D) Representative Wright-Giemsa stained cytospins of E14.5 PB. *Srsf2*$^{\Delta/\Delta}$ PB lacked definitive red blood cells. (E) Quantification of panel D. f/+, n = 4; f/f, n = 5; Δ/+, n = 8; and Δ/Δ, n = 7. * indicates $p < 0.05$; ** indicates $p < 0.005$.

Figure 4. Srsf2 is indispensable for survival of adult BM cells. (A) - (D) PolyIC injection into adult *Mx1Cre+ or - Srsf2* cKO mice. PolyIC was injected *i.p.* every other day for three times into cKO mice (600 μg/dose). The day of the first injection was defined as day 0. *Mx1Cre-Srsf2*$^{f/+}$, n = 11. *Mx1Cre-Srsf2*$^{f/f}$, n = 23. *Mx1Cre+Srsf2*$^{f/+}$, n = 9. *Mx1Cre+Srsf2*$^{f/f}$, n =

24. (A) Genotyping of PB and BM cells on day16. *Mx1Cre+Srsf2*$^{f/+}$samples showed almost complete excision of flox allele, while *Mx1Cre+Srsf2*$^{f/f}$ samples showed incomplete excision. (B) Platelet (Plt) count on day 16. (C) Total BM cells from femurs and tibias of both legs counted using Trypan blue. (D) Absolute number of LSK cells in total BM measured by flow cytometry. (E) LSK% in total BM measured by flow cytometry. (F) Competitive BMT of *Mx1Cre* cKO cells. One million test cells (CD45.2) were mixed with the same number of competitor cells (CD45.1) and transplanted. Chimerism in PB was evaluated by flow cytometry before (Week 0) and after polyIC injection. Five mice were in each group. *Mx1Cre+Srsf2*$^{f/f}$ cells had lower engraftment efficiency compared to others and showed continuous decrease of donor chimerism after polyIC injection. * indicates $p < 0.05$; ** indicates $p < 0.005$.

Figure 5. Overexpression of WT and mutant SRSF2 has similar phenotypes. (A) Protein expression of the overexpressed SRSF2 in mouse BM cells. β-actin serves as a loading control. Signal intensities of SRSF2 and loading control were used to calculate the relative SRSF2 expression level. (B) Growth curves of total BM cells in liquid culture. Mean and SD from three independent experiments are shown. All of WT-, P95H- and Δ8aa-expressing retrovirus transduced cells showed growth disadvantage compared to MIP control cells. (C) Apoptosis assay of cells on Day 3. Combined data of independent three experiments are shown. P95H and Δ8aa cells showed enhanced apoptosis compared to MIP and WT cells. (D) Colony forming assay. Combined data of three independent experiments are shown. (E) BMT of SRSF2 overexpressing cells. Bone marrow cells were transduced with MigR1 vector, MigR1-SRSF2 WT, and MigR1-SRSF2 P95H retrovirus. Two days after initial cell infection, cells were transplanted into lethally irradiated recipient mice. Five recipients were used in each

group. Representative result of three independent experiments is shown. MigR1 recipients had higher GFP% in PB compared to SRSF2 WT and P95H counterparts. * indicates $p < 0.05$; ** indicates $p < 0.005$.

Figure 6. Inducible low-level expression of mutant *SRSF2* causes apoptosis and growth arrest. (A) Structure of pTRIPZ-*SRSF2* constructs. Expression of microRNA-adapted shRNA against endogenous *SRSF2* (shRNA-mir) and cDNA of shRNA-resistant WT or mutant human *SRSF2* is driven by TRE. TRE, tetracycline inducible promoter. UBC, human ubiquitin C promoter. rtTA3, reverse tetracycline transactivator 3. IRES, internal ribosomal entry site. Puro-R, puromycin resistant gene. sinLTR, self-inactivating long terminal repeat. (B) Quantitative RT-PCR of *SRSF2*. The samples were measured in duplicate, and normalized to GAPDH. Expression in untreated WT cells was set to 1. 3'-UTR, endogenous *SRSF2* expression. Exon 2 CDS, exon 2 coding sequence representing total *SRSF2* expression. (C) Growth curves. Cells were seeded in triplicate in four independent experiments and counted with Trypan blue. Dox-treated P95H and Δ8aa cells showed significant growth suppression compared to other groups. (D) Apoptosis assay. Cells were seeded in duplicate in four independent experiments. Early apoptotic cells are defined as AnnexinV+ 7AAD- cells. Dox-treated P95H and Δ8aa cells showed significantly enhanced apoptosis compared to other groups. ** indicates $p < 0.005$.

Figure 7. Target genes of WT and mutant SRSF2 by RASL-seq analysis. (A) Unsupervised hierarchical clustering show that splicing events of WT, P95H and Δ8aa (Δ8) cells in the absence of Doxycycline (Dox -) are very similar and are separated from cells with activated

shRNA/*SRSF2* expression (Dox +) (Left panel). Δ8aa and P95H are grouped side by side, with Δ8aa showing stronger signal. Unsupervised hierarchical clustering of splicing events of ShSRSF2-only cells cultured in the presence or absence of Dox are also shown (right panel). Green: less short isoform, more long isoform; red: more short isoform, less long isoform. (B) Venn Diagram showing the overlap and difference of splicing events upon Dox activated expression of WT, P95H and Δ8aa *SRSF2* compared to shRNA only expression. (C) Venn Diagram showing significant overlapped events (487) from P95H and Δ8aa groups relative to WT SRSF2 group. Among these shared events, over 96% are in the same direction. For these significant events changed in the same direction, Δ8aa induced changes in 450 out of 470 events are over 1.5 fold compared to that in P95H induced events. (D) Validation of 10 selected RASL-seq events. Upper panel: heatmap demonstration of 10 RASL-seq events ratio (short isoform/long isoform). Green: less short isoform, more long isoform; red: more short isoform, less long isoform. Bottom panel: RT-PCR validation of 10 RASL-seq events.

Figure 8. Pathway and correlation studies of target genes of WT and mutant SRSF2. (A) Top biological functions of the 470 common and same direction targets of Δ8aa and P95H based on IPA. The –log(p value) means the significance of the functions to the data set. (B) Venn Diagram showing significant overlapped events of 470 common targets of P95H and Δ8aa over WT SRSF2 relative to cells expressing only shRNA. Events changed in the same or opposite directions are also listed separately.

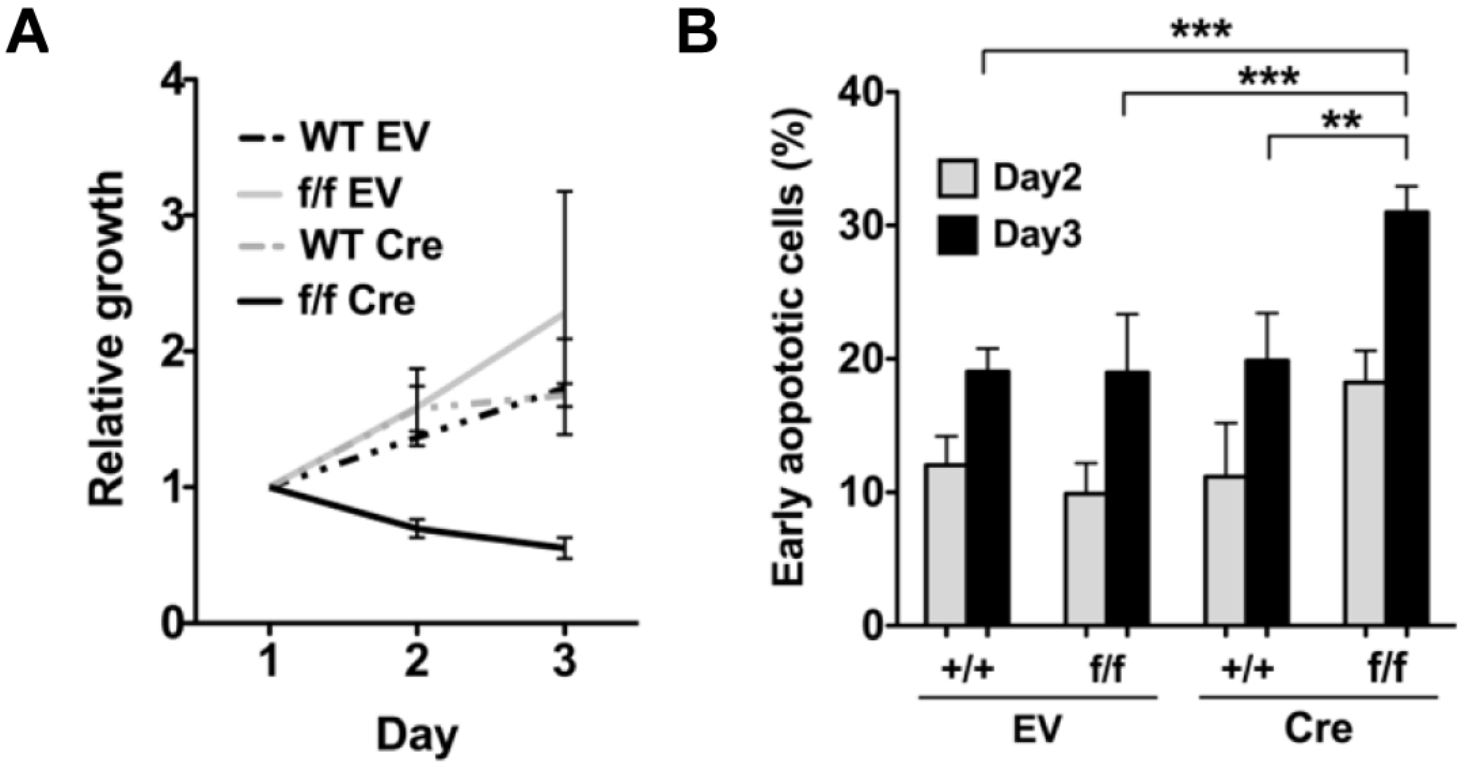
A
Relative growth
4
3
2
1
0
WT EV
f/f EV
WT Cre
f/f Cre
1
2
3
Day
B
Early aopototic cells (%)
40
30
20
10
0
***
***
**
Day2
Day3
+/+
f/f
+/+
f/f
EV
Cre

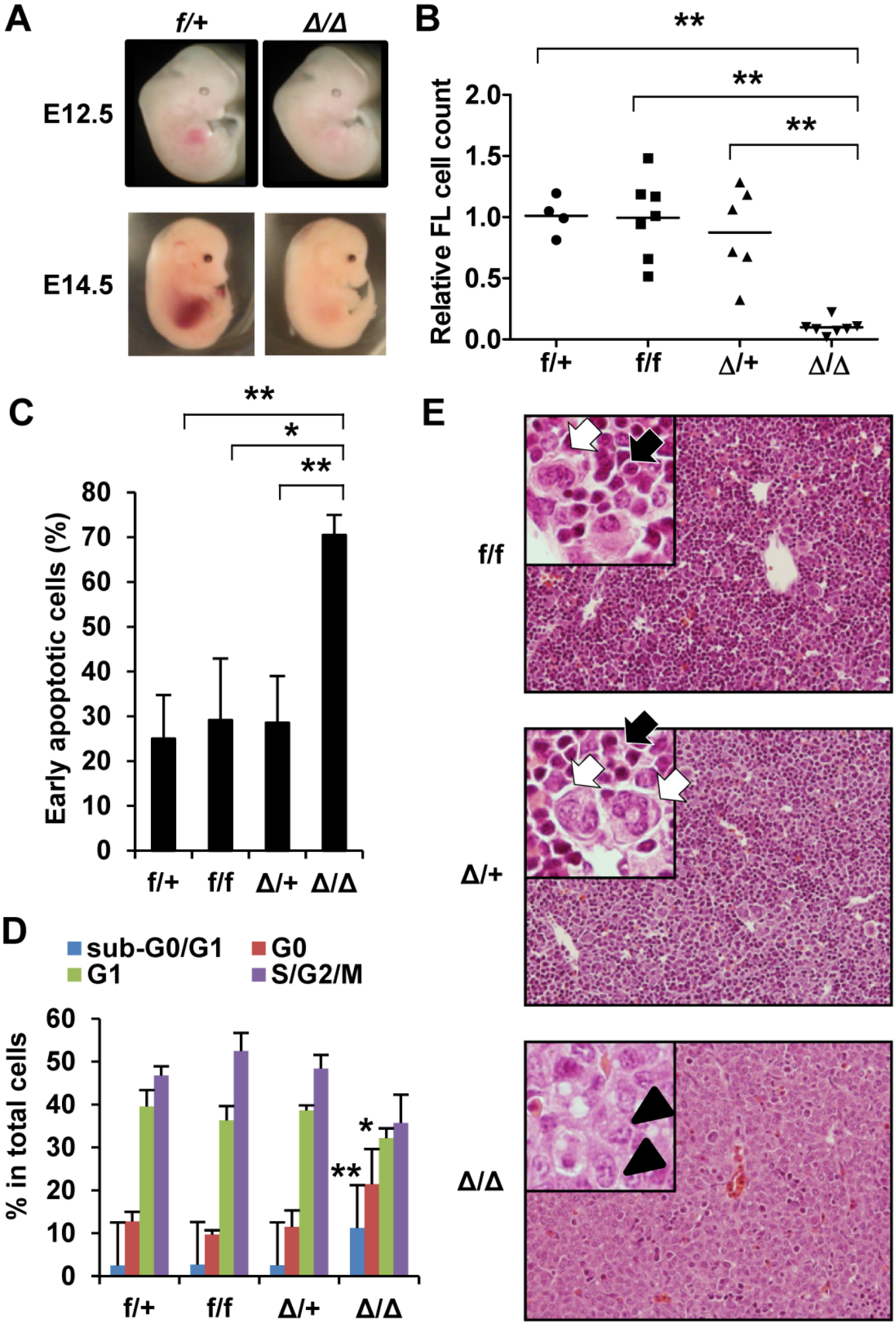
A
f/+
Δ/Δ
E12.5
E14.5
B
**
**
**
Relative FL cell count
2.0
1.5
1.0
0.5
0.0
f/+
f/f
Δ/+
Δ/Δ
C
**
*
**
Early apoptotic cells (%)
80
70
60
50
40
30
20
10
0
f/+
f/f
Δ/+
Δ/Δ
D
sub-G0/G1
G0
G1
S/G2/M
% in total cells
60
50
40
30
20
10
0
**
*
f/+
f/f
Δ/+
Δ/Δ
E
f/f
Δ/+
Δ/Δ

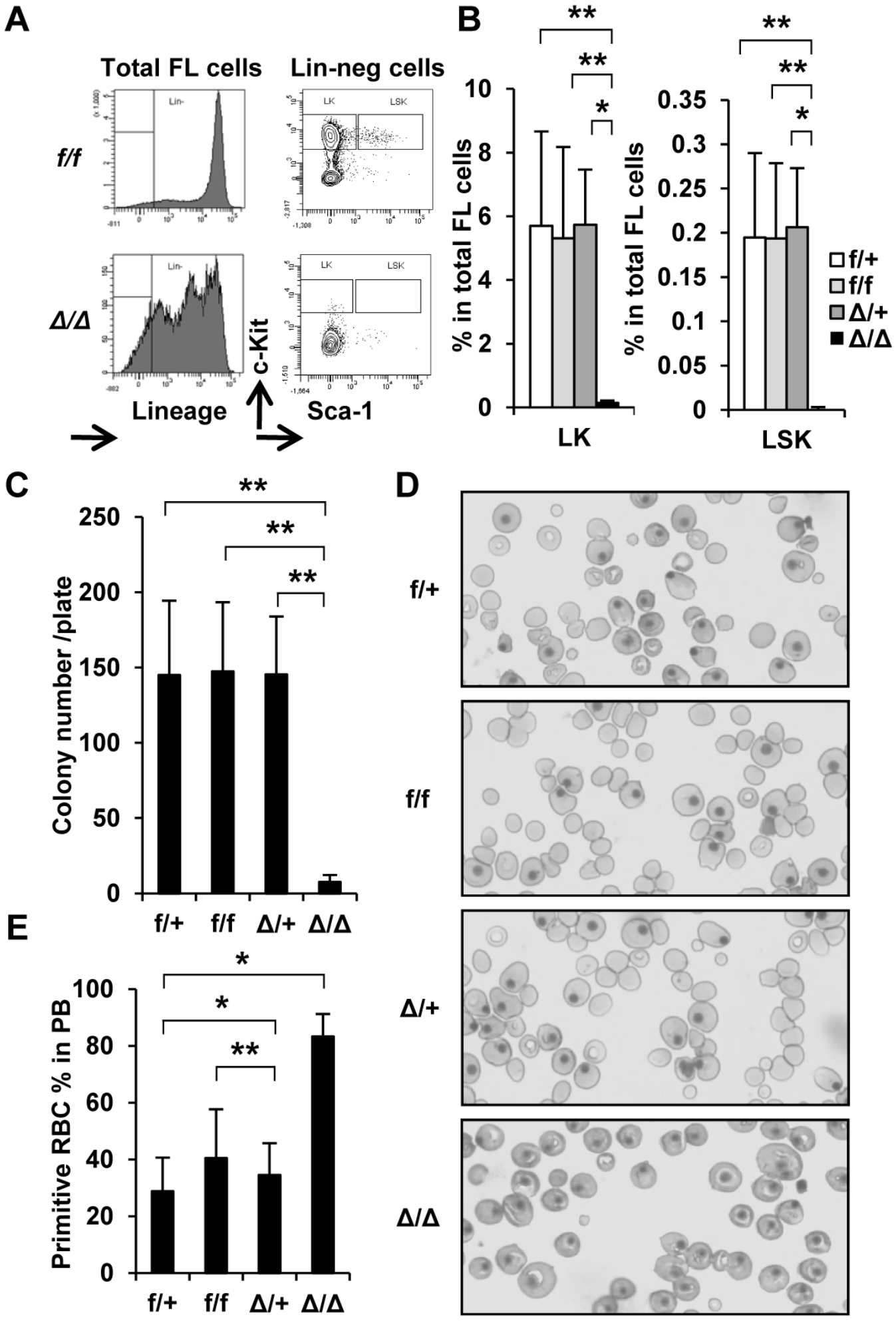
A
Total FL cells
Lin-neg cells
f/f
Δ/Δ
Lin-
LK
LSK
c-Kit
Lineage
Sca-1
B
% in total FL cells
LK
LSK
f/+
f/f
Δ/+
Δ/Δ
C
Colony number /plate
f/+
f/f
Δ/+
Δ/Δ
D
E
Primitive RBC % in PB

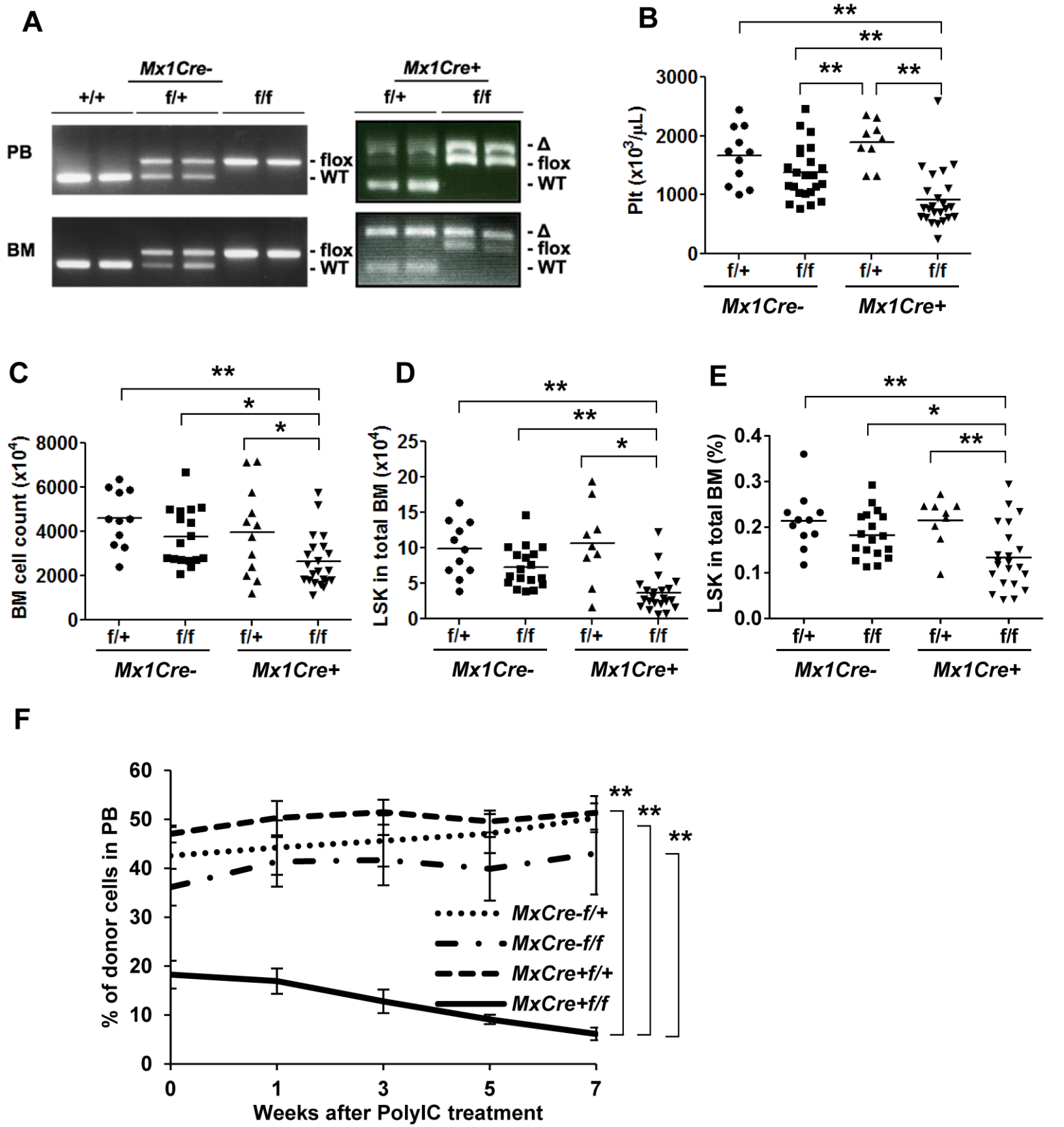
A
Mx1Cre-
Mx1Cre+
+/+
f/+
f/f
f/+
f/f
PB
BM
- flox
- WT
- Δ
- flox
- WT
B
Plt (x10^3/μL)
3000
2000
1000
0
**
**
**
**
f/+
f/f
f/+
f/f
Mx1Cre-
Mx1Cre+
C
BM cell count (x10^4)
8000
6000
4000
2000
0
**
*
*
f/+
f/f
f/+
f/f
Mx1Cre-
Mx1Cre+
D
LSK in total BM (x10^4)
25
20
15
10
5
0
**
**
*
f/+
f/f
f/+
f/f
Mx1Cre-
Mx1Cre+
E
LSK in total BM (%)
0.4
0.3
0.2
0.1
0.0
**
*
**
f/+
f/f
f/+
f/f
Mx1Cre-
Mx1Cre+
F
% of donor cells in PB
60
50
40
30
20
10
0
0
1
3
5
7
Weeks after PolyIC treatment
**
**
**
MxCre-f/+
MxCre-f/f
MxCre+f/+
MxCre+f/f

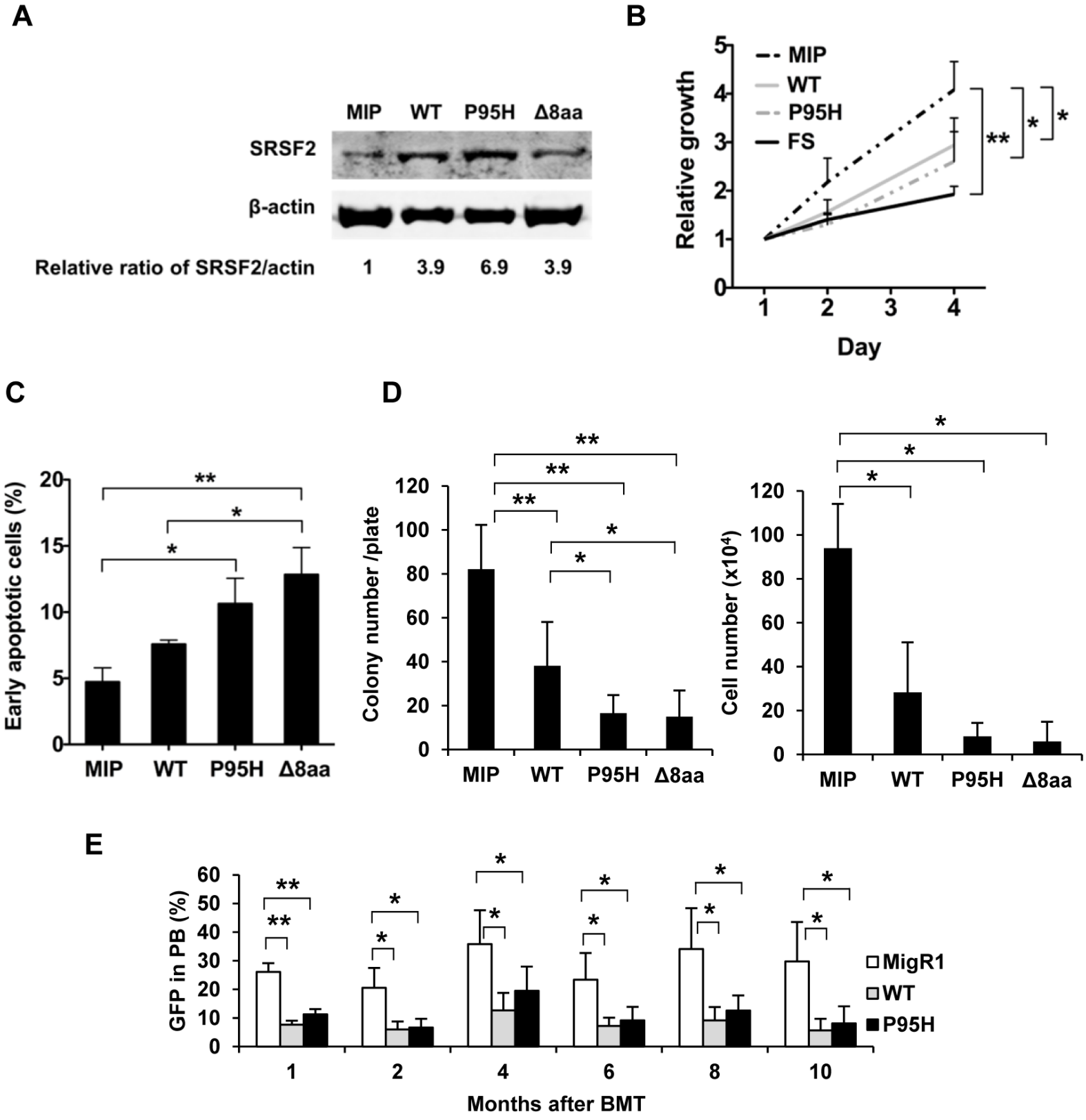
A
MIP
WT
P95H
Δ8aa
SRSF2
β-actin
Relative ratio of SRSF2/actin
1
3.9
6.9
3.9
B
MIP
WT
P95H
FS
Relative growth
Day
C
Early apoptotic cells (%)
D
Colony number /plate
Cell number (x10⁴)
E
GFP in PB (%)
MigR1
WT
P95H
Months after BMT

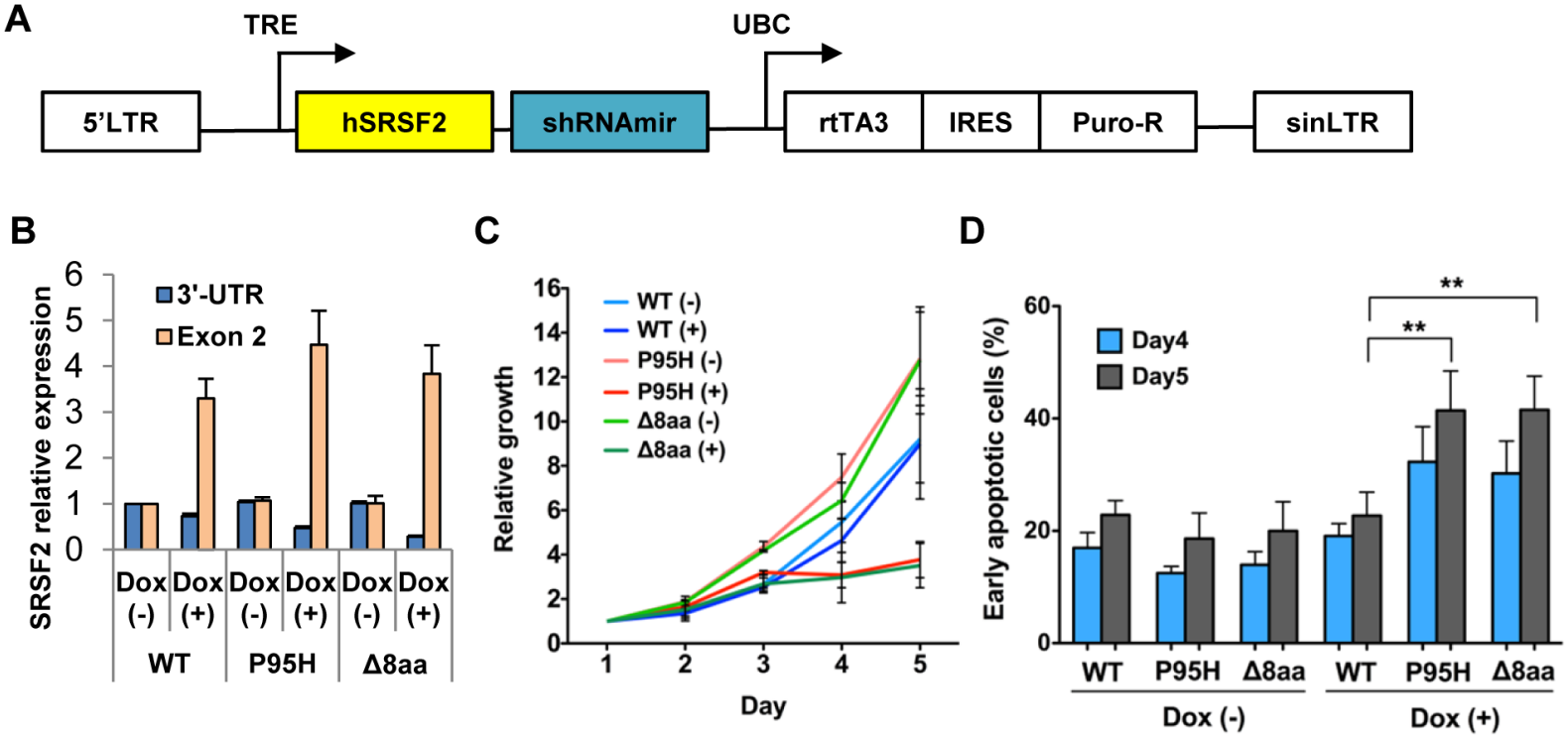
A
TRE
UBC
5'LTR
hSRSF2
shRNAmir
rtTA3
IRES
Puro-R
sinLTR
B
SRSF2 relative expression
3'-UTR
Exon 2
Dox (-)
Dox (+)
WT
P95H
Δ8aa
C
Relative growth
WT (-)
WT (+)
P95H (-)
P95H (+)
Δ8aa (-)
Δ8aa (+)
Day
D
Early apoptotic cells (%)
Day4
Day5
**
**
WT
P95H
Δ8aa
Dox (-)
Dox (+)

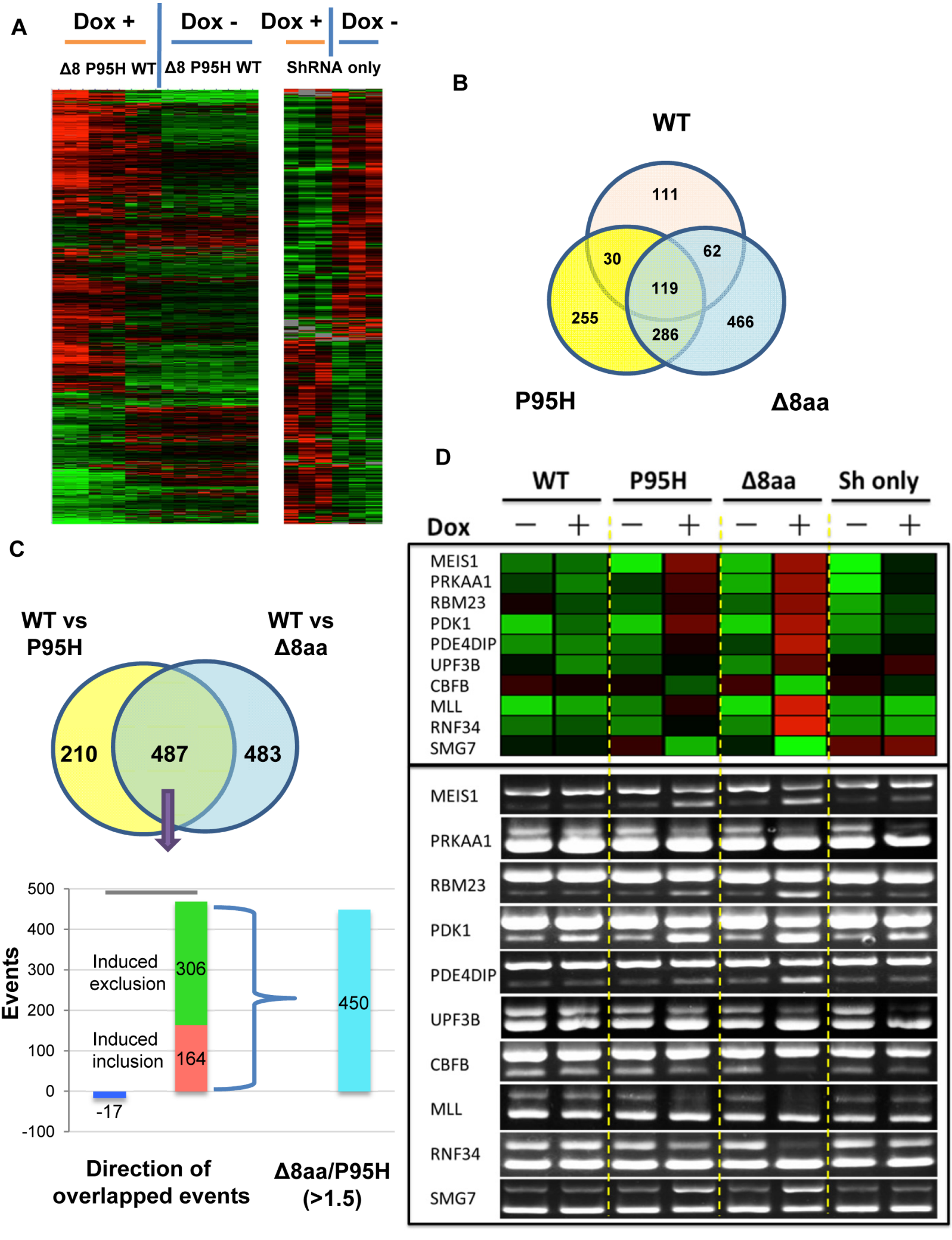
A
Dox +
Dox -
Dox +
Dox -
Δ8 P95H WT
Δ8 P95H WT
ShRNA only
B
WT
111
30
62
119
255
466
286
P95H
Δ8aa
C
WT vs P95H
WT vs Δ8aa
210
487
483
500
400
300
200
100
0
-100
Events
Induced exclusion
306
Induced inclusion
164
-17
450
Direction of overlapped events
Δ8aa/P95H (>1.5)
D
WT
P95H
Δ8aa
Sh only
Dox
− + − + − + − +
MEIS1
PRKAA1
RBM23
PDK1
PDE4DIP
UPF3B
CBFB
MLL
RNF34
SMG7

A

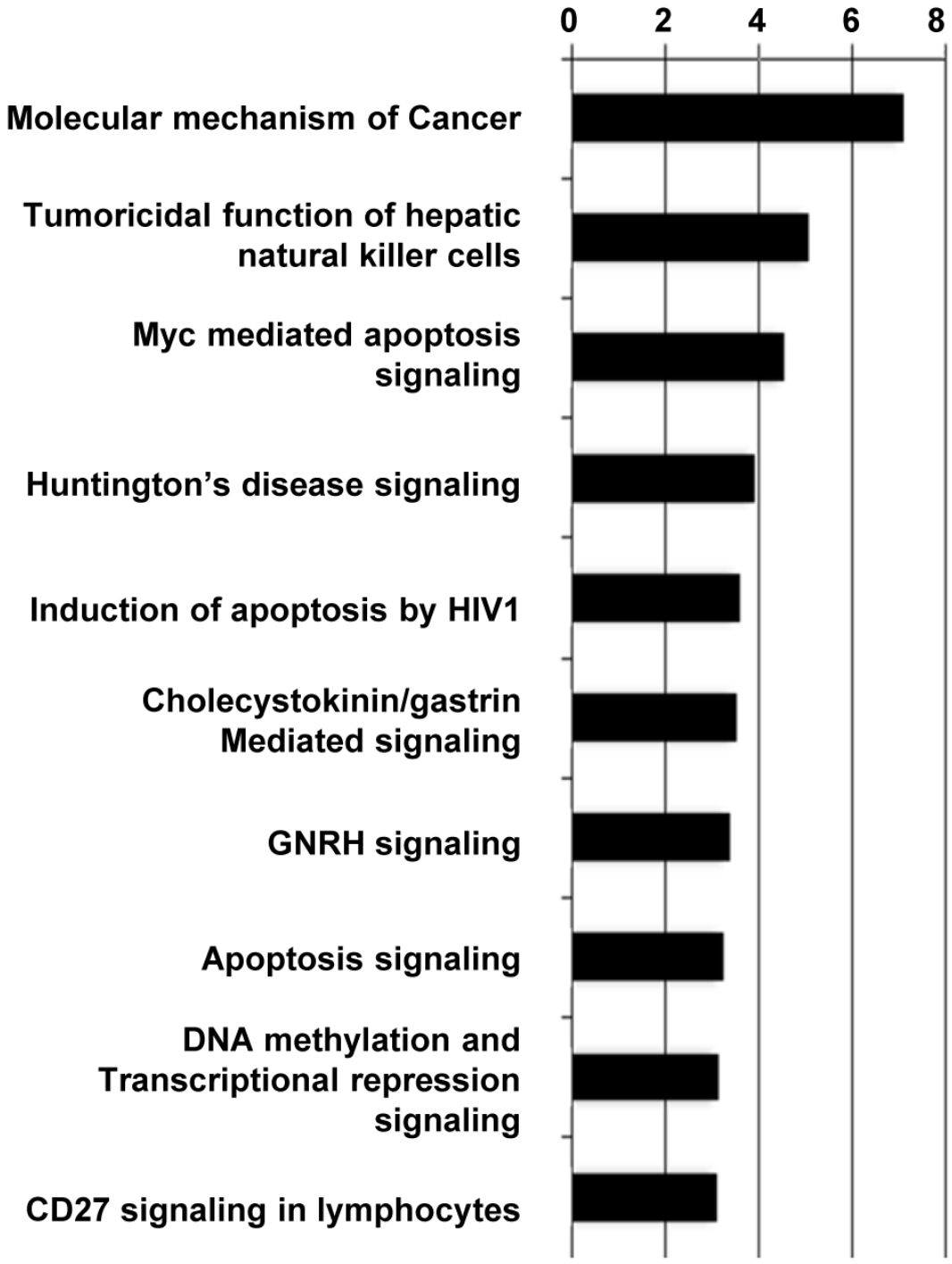
0
2
4
6
8
Molecular mechanism of Cancer
Tumoricidal function of hepatic natural killer cells
Myc mediated apoptosis signaling
Huntington's disease signaling
Induction of apoptosis by HIV1
Cholecystokinin/gastrin Mediated signaling
GNRH signaling
Apoptosis signaling
DNA methylation and Transcriptional repression signaling
CD27 signaling in lymphocytes

B

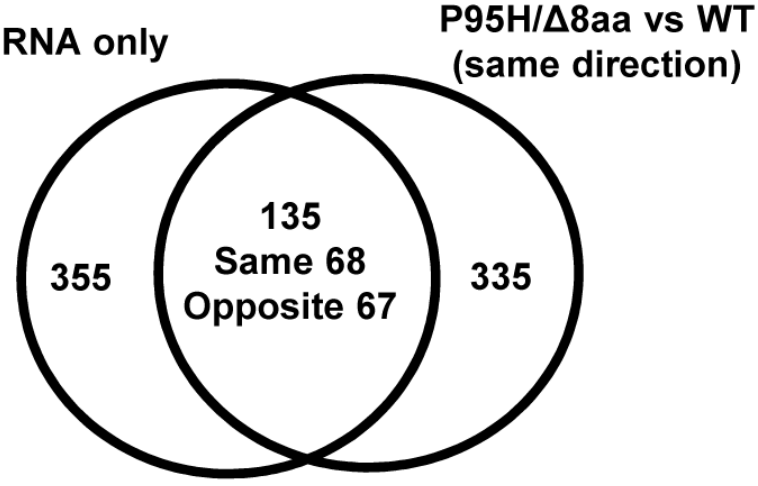
ShRNA only
P95H/Δ8aa vs WT (same direction)
355
135
Same 68
Opposite 67
335